Modulation of Human Arylamine N-Acetyltransferase 1 Activity by Lysine Acetylation: Role of p300/CREB-Binding Protein and Sirtuins 1 and 2 [S]

Neville J. Butcher, Rachel Burow, and Rodney F. Minchin

School of Biomedical Sciences, University of Queensland, St Lucia, Queensland, Australia

Received November 28, 2019; accepted April 22, 2020

ABSTRACT

Arylamine N-acetyltransferase 1 (NAT1) is a phase II xenobiotic-metabolizing enzyme that also has a role in cancer cell growth and metabolism. Recently, it was reported that NAT1 undergoes lysine acetylation, an important post-translational modification that can regulate protein function. In the current study, we use site-directed mutagenesis to identify K^{100} and K^{188} as major sites of lysine acetylation in the NAT1 protein. Acetylation of ectopically expressed NAT1 in HeLa cells was decreased by C646, an inhibitor of the protein acetyltransferases p300/CREB-binding protein (CBP). Recombinant p300 directly acetylated NAT1 in vitro. Acetylation of NAT1 was enhanced by the sirtuin (SIRT) inhibitor nicotinamide but not by the histone deacetylase inhibitor trichostatin A. Cotransfection of cells with NAT1 and either SIRT 1 or 2, but not SIRT3, significantly decreased NAT1 acetylation. NAT1 activity was evaluated in cells after nicotinamide treatment to enhance acetylation or cotransfection with SIRT1 to inhibit acetylation. The results indicated that NAT1 acetylation impaired its enzyme kinetics, suggesting decreased acetyl coenzyme A binding. In addition, acetylation attenuated the allosteric effects of ATP on NAT1. Taken together, this study shows that NAT1 is acetylated by p300/CBP in situ and is deacetylated by the sirtuins SIRT1 and 2. It is hypothesized that post-translational modification of NAT1 by acetylation at K^{100} and K^{188} may modulate NAT1 effects in cells.

SIGNIFICANCE STATEMENT

There is growing evidence that arylamine N-acetyltransferase 1 has an important cellular role in addition to xenobiotic metabolism. Here, we show that NAT1 is acetylated at K^{100} and K^{188} and that changes in protein acetylation equilibrium can modulate its activity in cells.

Introduction

Human arylamine N-acetyltransferase 1 (NAT1) is a drug-metabolizing enzyme that also has a role in cell growth and survival. This has led several investigators to postulate that NAT1 may be an important drug target. Like most proteins, expression of NAT1 is regulated at the transcriptional and post-transcriptional levels. Transcription occurs from multiple promoters that generate a number of mRNA splice variants (Husain et al., 2004; Butcher et al., 2005). The different promoters show tissue specificity (Barker et al., 2006; Husain et al., 2007), but all have an identical coding region (Butcher et al., 2008). Translational efficiency of the various splice variants is dependent on the length of the 5′ untranslated region (Butcher et al., 2005). Similar to many other genes, NAT1 transcription is altered by changes in histone acetylation (Paterson et al., 2011) and promoter methylation (Kim et al., 2008). In cancer cells, NAT1 transcription is induced by androgens (Butcher et al., 2007) but not

by estrogens (Zhang et al., 2018). Although there has been a growing understanding of the transcriptional control of NAT1, its regulation at the post-transcriptional level remains largely unknown.

Recent studies have suggested that NAT1 protein modifications regulate enzyme function. For example, alterations to lysine 100 (K^{100}) by site-directed mutagenesis decreased the affinity of the acetyl donor acetyl coenzyme A (AcCoA) for the protein (Minchin et al., 2018), suggesting it was important for AcCoA binding in the active site (Minchin and Butcher, 2015). K^{100} has also been associated with ATP binding to NAT1 (Minchin et al., 2018). ATP is an allosteric modulator and a competitive inhibitor of AcCoA binding to the enzyme. Ectopic expression of NAT1 where K^{100} was substituted by either arginine or glutamine clearly demonstrated that this amino acid is a target for acetylation (Minchin et al., 2018). Moreover, activators and inhibitors of the sirtuins (SIRTs), a family of protein deacetylases, have been used with peripheral blood mononuclear cells to identify possible effects of protein acetylation on the activity of NAT1 and the closely related NAT2 (Turiján-Espinoza et al., 2018). Although the study did not directly demonstrate changes in protein acetylation, it did detect higher NAT2 activity when the cells were treated with nicotinamide (NAM), an inhibitor of the sirtuins.

ABBREVIATIONS: AcCoA, acetyl coenzyme A; CBP, CREB-binding protein; KATs, lysine acetyltransferases; KDACs, lysine deacetylases; K_m, Michaelis-Menten constant; NAM, nicotinamide; NAT1, arylamine N-acetyltransferase 1; PABA, para-aminobenzoic acid; PBST, PBS containing 0.05% Tween-20; siRNA, small-interfering RNA; SIRTs, sirtuins; TSA, trichostatin A.

Taken together, these experiments suggest that lysine acetylation of NAT1 may be an important post-translational modification.

In the current study, lysine acetylation of NAT1 has been investigated in detail using site-directed mutagenesis, immunoprecipitation, and protein activity experiments to identify potential sites for NAT1 acetylation and their impact on enzymatic activity. In addition, the acetyltransferases and deacetylases that regulate NAT1 acetylation were investigated. Finally, kinetic studies showed that the acetylation of NAT1 reduced its enzymatic activity in situ.

Materials and Methods

Materials. Trichostatin A (TSA), NAM, β-nicotinamide adenine dinucleotide, NAD^+, AcCoA, para-aminobenzoic acid (PABA), ATP, DMSO, dithiothreitol, sodium butyrate, fatty acid free bovine serum albumin, EX-527 (6-Chloro-2,3,4,9-tetrahydro-1H-Carbazole-1-carboxamide), 3X FLAG peptide (F3799), anti-FLAG M2 affinity resin (A2220), anti-FLAG M2-peroxidase antibody (A8592), and cOmplete protease inhibitor cocktail were all purchased from Sigma-Aldrich (St Louis, MA). C646 (ab142163; 4-[4-[[5-(4,5-Dimethyl-2-nitrophenyl)-2-furanyl]methylene]-4,5-dihydro-3-methyl-5-oxo-1H-pyrazol-1-yl]benzoic acid) was from Abcam (Cambridge, UK). Human SIRT1 (SR308256B), SIRT2 (SR307890B), and universal scrambled (SR30004) small-interfering RNAs (siRNAs) were purchased from OriGene Technologies (Rockville, MD). Anti-SIRT1 (2496), anti-SIRT2 (12650), pan anti–acetylated-lysine (9441), and anti–α–tubulin (3873) antibodies were purchased from Cell Signaling Technology (Danvers, MA). Peroxidase-conjugated AffiniPure goat anti-rabbit (111-035-003) and anti-mouse (115-035-003) secondary antibodies were purchased from Jackson ImmunoResearch Laboratories (West Grove, PA). WESTAR Nova 2.0 chemiluminescent reagent was from Cyanagen (Bologna, Italy). Lipofectamine 2000 and RNAiMAX reagents were from Thermo Fisher Scientific (Waltham, MA). Human recombinant p300 (AG-40T-0023) was purchased from AdipoGen Life Sciences (San Diego, CA). Human recombinant SIRT1 (10011190) and SIRT2 (10011191) were from Cayman Chemical Company (Ann Arbor, MI). FLAG-tagged SIRTs 1–3 were gifts from Eric Verdin (plasmids 13812, 13813, 13814; Addgene) (North et al., 2003).

Cell Culture and Treatments. HeLa cells were obtained from the American Type Culture Collection (Manassas, VA) and cultured in RPMI 1640 medium supplemented with 5% fetal bovine serum (GE Healthcare Life Sciences, Parramatta, NSW, Australia), 2 mM L-glutamine, and penicillin/streptomycin (Thermo Fisher Scientific) at 37°C in a humidified 5% CO_2 atmosphere. Cells were treated with 20 μM C646 [p300/CREB-binding protein (CBP) inhibitor], 1 μM TSA (histone deacetylase inhibitor), 1 mM NAM (SIRT inhibitor), 1 μM EX-527 (SIRT1 inhibitor), or vehicle (DMSO) for 16 hours. HeLa cells were routinely tested for mycoplasma contamination using a MycoAlert mycoplasma detection kit (LT07-318; Lonza, Derrimut, VIC, Australia).

Plasmids and Transient Transfection. The p3XFLAG-CMV-7.1-NAT1 wild-type and $K^{100}Q$ mutant plasmids have been described previously (Butcher et al., 2004; Minchin and Butcher, 2015). To generate $K^{188}L$ and $K^{100}Q/K^{188}L$ mutant plasmids, the GENEART site-directed mutagenesis system (Thermo Fisher Scientific) was used with FP 5′-gacagcaaataccgacttatctactcctttact-3′ and RP 5′-agtaaagga gtagataagtcggtatttgctgtc-3′ and p3XFLAG-CMV-7.1-NAT1 wild-type or $K^{100}Q$ plasmids as template, respectively. Clones were verified by Sanger DNA sequencing.

HeLa cells were seeded at a density of 0.6×10^6 cells/well in six-well plates and allowed to adhere overnight. They were then transiently transfected with a total of 4 μg plasmid DNA using Lipofectamine 2000 according to the manufacturer's instructions. Where FLAG-NAT1 was cotransfected with SIRT plasmids, 3 and 1 μg were used,

respectively. Cells were transfected for a total of 48 hours. Drug treatments as described above were performed for the final 16 hours of transfection.

Transient siRNA Transfection. HeLa cells were seeded at a density of 0.6×10^6 cells/well in six-well plates and allowed to adhere overnight. They were then transiently transfected with a mixture of siRNAs directed against SIRT1 and SIRT2 (10 nM each) or 20 nM of scrambled negative control siRNA using Lipofectamine RNAiMAX according to the manufacturer's protocol. After 48 hours of siRNA transfection, cells underwent transfection with various FLAG-NAT1 plasmids as described above. After a further 24 hours of transfection, cells were washed twice with cold PBS and then lysed and immunoprecipitated with anti-FLAG M2 affinity resin as described below.

FLAG Immunoprecipitation and Protein Purification. After transfection, cells were washed twice with cold PBS and were lysed in 0.8 ml of FLAG lysis buffer (50 mM Tris, pH 7.4, 150 mM NaCl, 1 mM EDTA, and 1% Triton X-100) containing 1× protease inhibitor cocktail for 10 minutes on ice with shaking. Cell lysates were then transferred to microfuge tubes and were centrifuged at 16,000g for 10 minutes at 4°C. Supernatants were incubated with 30 μl of washed and equilibrated anti-FLAG M2 affinity resin for 1 hour at 4°C with rotation. The resin was sedimented by centrifugation at 6000g for 1 minute, washed with 1 ml of wash buffer (50 mM Tris, pH 7.4, 150 mM NaCl, 1 mM EDTA) three times, and boiled in 60 μl 1× Laemmli sample buffer for Western blot.

FLAG-NAT1 was purified from transiently transfected HeLa cells for use in the in vitro acetylation and deacetylation assays. Cells were transfected with FLAG-NAT1 (deacetylation assay) or FLAG-NAT1 and SIRT1 (acetylation assay), and then FLAG-NAT1 proteins were immunoprecipitated as described above. After the resin was washed three times, the FLAG-NAT1 was eluted from the resin using 3XFLAG peptide according to the manufacturer's protocol. Briefly, triplicate transfections were combined and immunoprecipitated with 100 μl of anti-FLAG M2 affinity resin. After washing, the resin was resuspended in 100 μl of wash buffer containing 3XFLAG peptide at a concentration of 100 μg/ml and slowly rotated at 4°C for 1 hour. The resin was briefly centrifuged, and the supernatant containing the eluted FLAG-NAT1 protein was removed and stored at 4°C until use.

Western Blotting. Protein samples were boiled for 5 minutes in 1× Laemmli sample buffer and were then separated by SDS-PAGE for 45 minutes at 200 V. Proteins were transferred to nitrocellulose membranes for 1 hour at 350 mA and were then blocked for 1 hour with 5% skim milk in PBS containing 0.05% Tween-20 (PBST). Membranes were washed three times with PBST and were then incubated with primary antibodies diluted 1:1000 in PBST overnight at 4°C. After washing with PBST, membranes were incubated with peroxidase-conjugated goat anti-mouse or anti-rabbit secondary antibodies diluted 1:30,000 in PBST for 1 hour and were then washed with PBST. Detection was performed by using WESTAR Nova 2.0 ECL reagent.

In Vitro Acetylation and Deacetylation Reactions. In vitro acetylation assays were performed using deacetylated FLAG-NAT1 purified from transfected HeLa cells as outlined above. Recombinant p300 protein (200 ng) was diluted in 120 μl of acetyltransferase assay buffer (50 mM Tris, pH 7.6, 0.1 mM EDTA, 10 mM Na butyrate, 1 mM dithiothreitol, 10% glycerol) containing 1× protease inhibitor cocktail and then was divided into two 60-μl aliquots. FLAG-NAT1 (200 ng) was added to one aliquot, and an equal volume of elution buffer was added to the other. Both were then made up to 90 μl with acetyltransferase assay buffer and then divided into 45-μl aliquots. AcCoA (5 μl of a 10-mM stock) was added to one aliquot of each condition, whereas the remaining aliquots had an equal volume of acetyltransferase assay buffer added. The final reaction volume was 50 μl, with the test reaction containing 50 ng of p300 protein, 100 ng of FLAG-NAT1, and 1 mM of AcCoA. Reaction mixtures were incubated for 1 hour at 30°C, after which time 25 μl of 3× Laemmli sample buffer was added and samples were boiled for 5 minutes. Samples (20 μl) were then subjected to Western blot as described above.

In vitro deacetylation assays were performed by using purified FLAG-NAT1 and recombinant SIRT1 and SIRT2 proteins. Reactions contained 100 ng of FLAG-NAT1 in sirtuin assay buffer (50 mM Tris, pH 8.0, 137 mM NaCl, 2.7 mM KCl, 1 mM MgCl$_2$, 1 mg/ml fatty acid free bovine serum albumin), 0.5 mM of NAD+, and 30 ng of either SIRT1 or SIRT2 recombinant protein. Some reactions also contained 1 μM of the SIRT1/2 inhibitor EX-527. Reactions were incubated for 1 hour at 37°C, after which 25 μl of 3× Laemmli sample buffer was added and samples were boiled for 5 minutes. Samples (20 μl) were then subjected to Western blot as described above.

NAT1 Activity Assay. NAT1 activity was assayed by using PABA as acetyl acceptor and AcCoA as the acetyl donor. N-acetyl-PABA was measured by high-performance liquid chromatography as previously described (Tiang et al., 2011). Kinetic parameters for PABA were determined by using 1100 μM of AcCoA and 0–1200 μM of PABA. All reactions were performed under linear conditions with respect to substrate and protein. NAT1 activities were normalized for protein expression using FLAG Western blots of each cell lysate.

Data Analysis. Data are presented as means ± S.D. from three independent experiments unless otherwise stated. Western blot images were quantified by densitometry using ImageJ software, and statistical comparisons were performed with GraphPad Prism 7 (GraphPad Software, La Jolla, CA) using one-way ANOVA (with Bonferroni's correction for multiple tests) or Student's t test as indicated. Kinetic parameters were estimated by nonlinear least squares regression, using GraphPad Prism 7 with the following equation:

$$\text{Activity} = V\text{max}*S/(Km + S*(1 + S/Ki))$$

where S = concentration of PABA, V_{max} = maximum velocity, K_m = Michaelis-Menten constant, and K_i = substrate inhibition constant. Convergence was confirmed using three independent initial values. This was an exploratory study that did not set out to test a prespecified statistical null hypothesis. Consequently, P values should be interpreted as descriptive. All sample sizes were determined before experiments were performed.

Crystal Structure Analysis. The crystal structure coordinates (2PQT) for NAT1 were obtained from the Brookhaven protein database and visualized by using Swiss PDB Viewer version 4.0.1 (Swiss Institute of Bioinformatics).

Results

Identification of Lysine Residues in NAT1 that are Subject to Post-Translational Acetylation. It has previously been reported that NAT1 K[100] is acetylated. This amino acid is adjacent to a second lysine located at position 99 and is located in close proximity to K[188] (Fig. 1A). The crystal structure of NAT1 (Brookhaven protein database 2PQT; resolution 1.78 Å) was used to identify the spatial arrangement of K[100] and K[188] at the surface of the protein (Wu et al., 2007). K[100] is located at the opening to the active site of the enzyme and is thought to interact with the 3′-phosphoanion on the AcCoA molecule (Minchin and Butcher, 2015). K[188] is in close proximity to K[100] but further away from the active site. The exact distance between the two sidechains could not be determined, as the K[100] sidechain is missing from the crystal structure. Nevertheless, their proximity indicates the possibility of an interaction between the two. Mutation of either K[100] or K[188] significantly ($P < 0.005$, ANOVA) reduced overall protein acetylation by 60%–100% (Fig. 1B). However, mutation of K[99], or a range of other lysine residues, did not affect overall protein acetylation (Supplemental Data). These results suggested that K[100] and K[188] are the major sites for NAT1 lysine acetylation. To confirm this, both amino acids
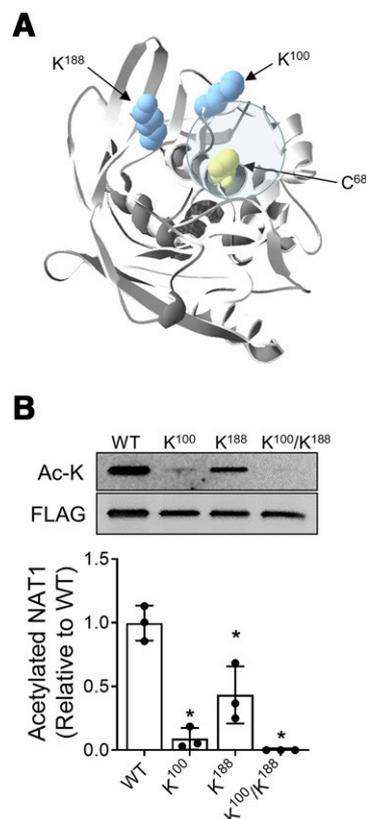

Fig. 1. Acetylation of lysine residues in NAT1. (A) Structure of NAT1 showing the orientation of K[100] near the entry to the active site and K[188]. The active site cysteine (C[68]) is also shown. (B) HeLa cells were transfected with FLAG-tagged NAT1 wild-type (WT), K[100] mutant, K[188] mutant, or K[100]/K[188] double-mutant plasmids, and then FLAG-tagged proteins were immunoprecipitated using FLAG M2 affinity resin. FLAG-tagged proteins were Western blotted with pan anti–acetyl-lysine (Ac-K) or anti-FLAG antibodies. Western blots were quantified by densitometry, and acetylated NAT1 was normalized to total immunoprecipitated FLAG protein and expressed relative to WT. A representative Western blot is shown above the graph. Data are means ± S.D., $n = 3$. Asterisks indicate significant difference compared with WT (ANOVA with Bonferroni's correction for multiple tests, $P < 0.05$).

were mutated together, resulting in almost complete loss of acetylated protein (Fig. 1B).

NAT1 is Acetylated by the Lysine Acetyltransferase p300/CBP. The lysine acetyltransferases (KATs) CBP and p300, also known as KAT3A and KAT3B, respectively, are localized both to the nucleus and cytosol. The cell-permeable competitive inhibitor of p300/CBP, C646, was used to determine if this family of KATs was able to acetylate NAT1 in whole cells. HeLa cells transfected with FLAG-NAT1 were treated with either 20 μM of C646 or vehicle (DMSO) for 16 hours, and then NAT1 was immunoprecipitated with FLAG M2 affinity resin. Western blot using a pan anti–acetyl-lysine antibody showed cells treated with C646 had 62% less acetylated NAT1 compared with vehicle-treated controls ($P = 0.006$, Student's t test, Fig. 2A).

To determine whether p300 could directly acetylate purified NAT1 protein, recombinant p300 protein was used in an in vitro acetylation assay. Reactions containing 50 ng of recombinant p300 protein in the presence or absence of cofactor (AcCoA) and purified NAT1 proteins were incubated for 1 hour at 30°C. The resulting Western blot of the proteins in the assay

A

B
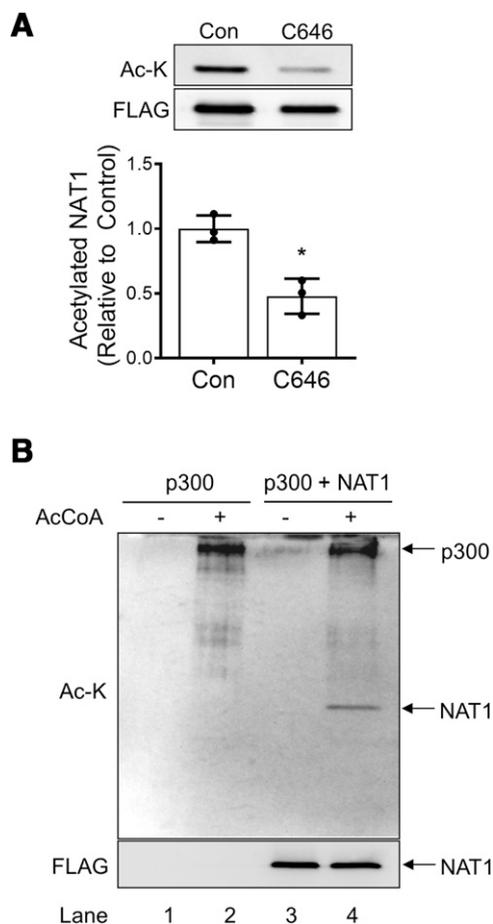
Fig. 2. Acetylation of NAT1 by p300/CBP. (A) Acetylation of NAT1 in whole cells. HeLa cells were transiently transfected with FLAG-NAT1 and treated with 20 μM of C646 or vehicle (DMSO) for 16 hours. Cells were then lysed, and FLAG-NAT1 protein was immunoprecipitated using FLAG M2 affinity resin and Western blotted for acetylated NAT1 (Ac-K) and total NAT1 protein (FLAG). Acetylated NAT1 was quantified by densitometry and normalized to total NAT1 protein. A representative Western blot is shown above the graph. Results are mean $\pm$ S.D., $n = 3$. $*P < 0.05$ (Student's t test, significant difference). (B) In vitro acetylation of NAT1 by recombinant p300. Purified FLAG-NAT1 protein was incubated with recombinant p300 in the presence or absence of 1 mM of AcCoA for 1 hour at 30°C. Reactions were boiled in Laemmli buffer and subjected to Western blot with pan anti–acetyl-lysine (Ac-K) and anti-FLAG antibodies. The positions of p300 and NAT1 are shown.

demonstrated the expected autoacetylation of p300 in the presence of AcCoA (Fig. 2B, lanes 2 and 4). In addition, when NAT1 was added to the reaction, acetylated NAT1 protein was detected (Fig. 2B, lane 4). These experiments suggest p300/CBP can directly acetylate NAT1 in vitro and in situ.

Deacetylation of NAT1. The acetylation status of a protein is the net effect of KATs and lysine deacetylases (KDACs). There are two families of KDACs: histone deacetylases, which are Zn^{2+}-dependent and inhibited by TSA, and SIRTs, which are NAD^+-dependent and inhibited by NAM. To determine which KDAC was involved in the deacetylation of NAT1, HeLa cells transfected with FLAG-NAT1 were treated with either 1 μM of TSA or 1 mM of NAM for 16 hours. Cells were lysed, NAT1 protein was immunoprecipitated with anti-FLAG M2 affinity resin, and acetylation was determined by Western blot using a pan anti–acetyl-lysine antibody. Total immunoprecipitated NAT1 was blotted with anti-FLAG antibody for

normalization. Treatment with NAM significantly increased the acetylation of NAT1 by approximately fourfold ($P < 0.001$, ANOVA), whereas treatment with TSA had no effect (Fig. 3A).

NAT1 is predominantly localized to the cytoplasm, but it has also been observed in the nucleus (Butcher et al., 2007). SIRT2 is the predominant sirtuin in the cytoplasm, whereas SIRT1 is known to shuttle out of the nucleus into the cytoplasm. SIRT3 is localized to the mitochondria. To determine which of the sirtuins were able to deacetylate NAT1, HeLa cells were cotransfected with FLAG-NAT1 and either SIRT1, SIRT2, or SIRT3. FLAG proteins were immunoprecipitated and subjected to Western blot as above. The results showed that both SIRT1 and SIRT2 led to the deacetylation of NAT1 in situ, whereas SIRT3 had no effect (Fig. 3B). To confirm that either SIRT1 or SIRT2 could directly deacetylate NAT1, acetylated FLAG-NAT1 was produced in HeLa cells and purified by immunoprecipitation. Recombinant SIRT1 and 2 in the presence of the cofactor NAD^+ decreased the amount of NAT1 acetylation by 80% and 50%, respectively (Fig. 3C). This loss of acetylated NAT1 was prevented by the addition of the SIRT1/2 inhibitor EX-527 to the reactions.

To provide further evidence that SIRT1 and SIRT2 were able to deacetylate NAT1 in whole cells, endogenous SIRT1 and 2 were knocked down simultaneously by using siRNA. After 48 hours of SIRT knockdown, HeLa cells were transfected with FLAG-NAT1 WT, K^{100} mutant, or K^{100}/K^{188} double-mutant plasmids. Cells were lysed, NAT1 protein was immunoprecipitated with anti-FLAG M2 affinity resin, and acetylation was determined by Western blot. The effect of the siRNA on SIRT1 and SIRT2 expression was confirmed by Western blot (Fig. 4A). Knockdown of SIRT1/2 resulted in a 3.3-fold increase in acetylation for wild-type ($P = 0.004$, Student's t test) and a 2.5-fold increase in acetylation for K^{100} mutant ($P = 0.03$, Student's t test) NAT1 compared with the scrambled siRNA negative control (Fig. 4B). No acetylation of the K^{100}/K^{188} double-mutant NAT1 protein was evident with or without SIRT knockdown.

Effect of Acetylation on NAT1 Enzymatic Activity. To investigate whether the acetylation status of NAT1 affects its activity, HeLa cells were transiently transfected with FLAG-NAT1 with or without SIRT1 to minimize acetylation of NAT1 (Fig. 5A). Transfected cells were also treated with NAM to increase acetylation of NAT1 as shown in Fig. 3A. Consequently, SIRT1 cotransfection was used to establish minimum acetylation of NAT1, whereas NAM treatment was used to establish enhanced acetylation. The effects of each treatment on NAT1 enzyme activity was then assessed and is shown in Fig. 5, B and C. Switching from the acetylated to the non-acetylated state resulted in an increase in NAT1 activity (Fig. 5B). This was the result of an increase in the maximum velocity without a change in the K_m (Table 1). Moreover, the substrate inhibition constant was greater for NAT1 in the acetylated state. The kinetics for PABA acetylation were also quantified by using variable AcCoA concentrations (Fig. 5C). Under these conditions, there was an increase in the K_m without a change in maximum velocity (Table 2). These kinetic changes are similar to those reported earlier in which the charge on K^{100} was changed by using site-directed mutagenesis (Minchin and Butcher, 2015). Taken together, the results in Fig. 5, B and C suggest that acetylation of NAT1 impairs the binding of AcCoA to the enzyme.

ATP was recently reported to allosterically impair NAT1 activity, which was dependent on the presence of K^{100}

A

B

C

[1.0] [0.2] [1.1] [0.5] [0.9]
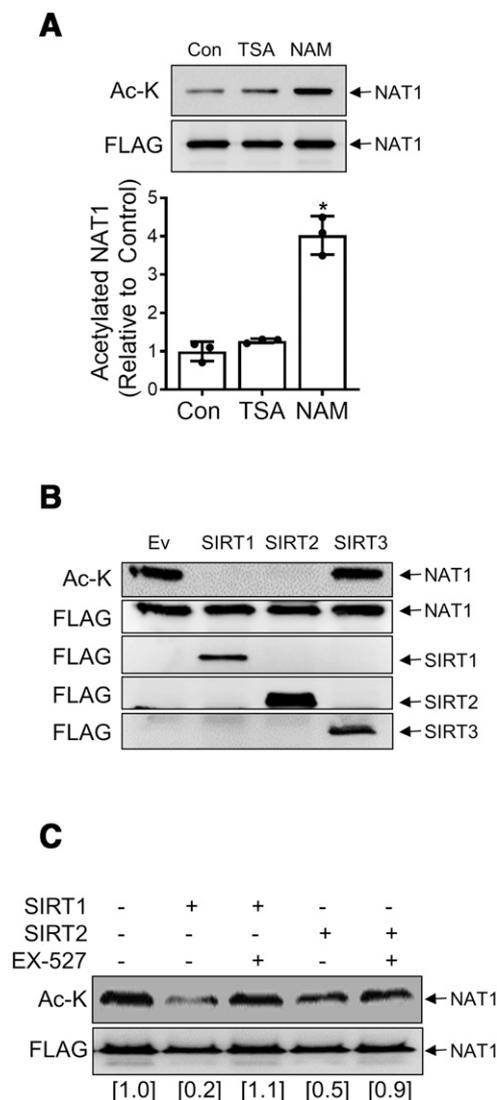
Fig. 3. Deacetylation of NAT1 by sirtuins. (A) Effect of TSA and NAM on NAT1 acetylation. HeLa cells were transiently transfected with FLAG-NAT1 and were treated with either 1 μM of TSA or 1 mM of NAM for 16 hours. Cells were lysed and FLAG-NAT1 was immunoprecipitated using anti-FLAG M2 affinity resin. Immunoprecipitates were then subjected to Western blot with pan anti–acetyl-lysine (Ac-K) and anti-FLAG antibodies. Acetylated NAT1 was quantified by densitometry, normalized to total immunoprecipitated FLAG protein, and expressed relative to untreated control (Con) samples. Data are presented as means ± S.D. from three independent experiments. A representative Western blot is shown above the graph. *$P < 0.05$ (significant difference) compared with control (ANOVA with Bonferroni's correction for multiple tests). (B) HeLa cells were transiently cotransfected with FLAG-NAT1 and either FLAG-SIRT1 (SIRT1), FLAG-SIRT2 (SIRT2), FLAG-SIRT3 (SIRT3), or FLAG empty vector (Ev). Cells were lysed and FLAG-tagged proteins immunoprecipitated using anti–FLAG M2 affinity resin. Immunoprecipitates were then Western blotted using pan anti–acetyl-lysine (Ac-K) and anti-FLAG antibodies. (C) In vitro deacetylation of FLAG-NAT1 by recombinant SIRT1 and SIRT2. Purified FLAG-NAT1 protein was incubated alone (−) or with recombinant SIRT1 or SIRT2 in the presence and absence of 1 μM of EX-527. Reactions contained 0.5 mM of NAD+ and were incubated for 1 hour at 37°C and then subjected to Western blot using pan anti–acetyl-lysine (Ac-K) and anti-FLAG antibodies. Acetylated NAT1 was quantified by densitometry, normalized to total FLAG-NAT1 protein, and expressed relative to NAT1 alone (shown in parentheses, n = 1).

(Minchin et al., 2018). In cells transfected with NAT1 alone, ATP (1 mM) decreased enzymatic activity in cytosolic preparations by 40% from 35 ± 3 to 21 ± 0.5 nmol/min per density

A

B
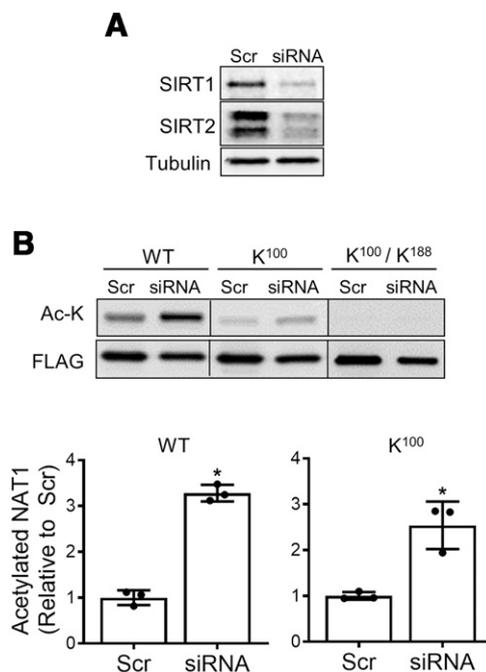
Fig. 4. Knockdown of SIRTs with siRNA increased NAT1 acetylation. (A) HeLa cells were transfected with either a mix of siRNAs (10 nM of each) directed against SIRTs 1 and 2 (siRNA) or with 20 nM of a scrambled control siRNA (Scr) for a total of 72 hours. SIRT1 and 2 knockdown with siRNA was confirmed by Western blot. (B) For the final 24 hours of the SIRT knockdown, cells were transiently transfected with either FLAG-tagged NAT1 (WT), K^{100} mutant, or K^{100}/K^{188} double-mutant plasmids. FLAG-tagged proteins were immunoprecipitated using FLAG-M2 affinity resin and Western blotted with pan anti–acetyl-lysine (Ac-K) or anti-FLAG antibodies. Acetylated NAT1 was quantified by densitometry, normalized to total immunoprecipitated FLAG protein, and expressed relative to Scr-treated samples. Data are presented as means ± S.D., $n = 3$. Representative Western blots are shown above the graphs. *$P < 0.05$ (Student's t test, significant difference).

unit (Fig. 5D, $P = 0.001$, ANOVA). When K^{100} was mutated to a glutamine, ATP had only a minor effect on NAT1 activity (15% decrease, $P = 0.04$) consistent with a role for K^{100} in ATP modulation of NAT1 activity. Furthermore, ATP inhibited NAT1 activity in cytosolic preparations from cells cotransfected with SIRT1 by 25% ($P = 0.0012$, ANOVA) but not from cells treated with NAM (Fig. 5E). These results suggest that deacetylation of NAT1 may enhance the allosteric effects of ATP on enzyme activity, although acetylation may inhibit these effects.

Estimation of the Fraction of NAT1 Acetylated In Situ. Because the activity of NAT1 is a function of its unacetylated state (Fig. 5B), these figures can be used to estimate the fraction of protein acetylated under normal conditions. Enzyme activity for NAT1-transfected cells, NAT1 plus SIRT1–transfected cells, and NAT1-transfected cells treated with NAM were plotted against the level of Ac-NAT1 protein normalized to total NAT1 protein (Figs. 3A and 5A). The addition of SIRT1 resulted in near complete deacetylation of the enzyme (Figs. 3B and 5A). Under these conditions, NAT1 activity was greatest (Fig. 5E). A single exponential decay was applied to the data, which estimated an asymptote at approximately 28 nmol/min per density unit. The asymptote predicts the activity of NAT1 when it is completely acetylated, which is very similar to that measured after treatment with NAM (29.2 nmol/min per density unit),

A

B

C

D

E

F
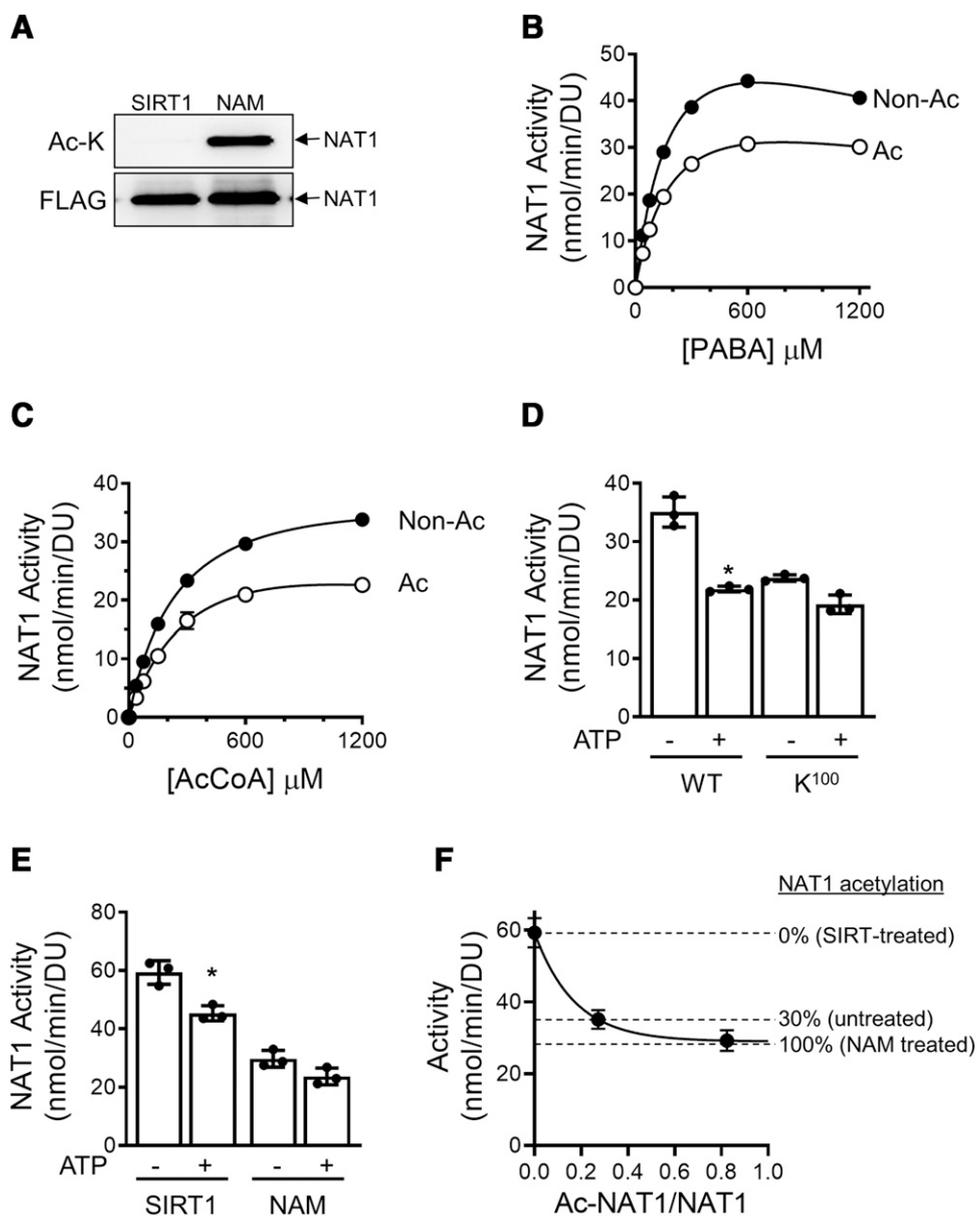
Fig. 5. Effect of acetylation on NAT1 kinetics. (A) HeLa cells were transiently transfected with FLAG-tagged NAT1 with or without SIRT1. After 24 hours, cells transfected with NAT1 alone were treated with 1 mM NAM for 16 hours. Acetylated NAT1 (Ac-K) and total NAT1 (FLAG) were identified as described in Fig. 1. (B) Metabolism of PABA by NAT1 in its nonacetylated (+SIRT1) and acetylated (+NAM) state. AcCoA was constant at 1 mM. Data were fitted to the Michaelis-Menten equation that included substrate inhibition, and the resulting curves are shown by the solid lines. (C) Metabolism of PABA with variable AcCoA by NAT1 in its nonacetylated (+SIRT1) and acetylated (+NAM) state. PABA was constant at 420 μM, and data were fitted as for (B). (D) Effects of the allosteric modulator ATP on NAT1 activity. Metabolism of PABA (420 μM) by wild-type (WT) and mutant (K^{100}) NAT1 in the absence and presence of 1 mM of ATP. (E) Effect of ATP on activity of acetylated (+NAM) and nonacetylated (+SIRT1) NAT1, as for (D). All data are means ± S.D., n = 3. *P < 0.05, significant difference between minus and plus ATP for each respective condition (ANOVA with Bonferroni's correction for multiple tests). (F) NAT1 activity vs. the ratio of acetylated to total NAT1. Data are means ± S.D., n = 3. DU, density units obtained from quantification of Western blots.

suggesting that near maximal acetylation was achieved with NAM treatment. Based on that assumption, the fraction of NAT1 acetylated in HeLa cells without any treatments can be estimated from the relative level of acetylated-NAT1 compared with that in NAM-treated cells. This indicated that approximately 30% of the protein was acetylated under control conditions. This estimate is in close agreement with the relative levels of acetylated NAT1 quantified in Fig. 3A.

Discussion

In this study, K^{100} and K^{188} were identified as major sites for NAT1 post-translational modification. These two amino acids reside in close proximity on the surface of NAT1, with K^{100} near the opening to the active site of the enzyme. Their closeness suggests that they may interact after acetylation or that they may compete for the activated acetyl moiety of the acetyltransferase. The K^{100}/K^{188} double mutation always

TABLE 1
Kinetic parameters for *p*-aminobenzoic acid acetylation by NAT1 with constant AcCoA (1 mM)

Condition	V_{max} (nmol/min per Density Unit)	K_m (μM)	K_i (mM)
Nonacetylated	72 ± 2	212 ± 10	2.01 ± 0.15
Acetylated	47 ± 1[a]	211 ± 6	2.92 ± 0.18[a]

[a]P < 0.01 compared with nonacetylated enzyme by Student's *t* test with 19 degrees of freedom.

TABLE 2
Kinetic parameters for *p*-aminobenzoic acid acetylation by NAT1 with variable AcCoA

Condition	V_{max} (nmol/min per density unit)	K_m (μM)
Nonacetylated	45 ± 2	273 ± 17
Acetylated	40 ± 4	407 ± 58[a]

[a]P < 0.01 compared with nonacetylated enzyme by Student's *t* test with 19 degrees of freedom.

showed a very faint acetylated lysine band of correct molecular weight (Figs. 1B and 4B) in Western blots, suggesting that other lysines may undergo acetylation, albeit to a lesser extent. Both K^{100} and K^{188} are conserved in human NAT2 as well as the NATs from other species. This suggests that the post-translational modification described here may be applicable more widely to other NATs.

p300/CBP was identified as one of the KATs that could catalyze NAT1 acetylation. This was confirmed both in vitro and in whole cells. Treatment of cells with the p300/CBP inhibitor C646 for 16 hours significantly decreased the level of NAT1 acetylation, but it did not completely abolish it. This may have been because of incomplete inhibition of the KATs by C646 or the presence of another acetyltransferase capable of acetylating NAT1. p300/CBP acetylates a wide range of substrates that show little structural similarity (Dancy and Cole, 2015). Figure 1A indicates that K^{100} or K^{188} can be acetylated in the absence of the second lysine, suggesting p300/CBP acetylates each site independently. Although changes to K^{100} have been associated with reduced enzyme activity, primarily through changes in AcCoA binding (Minchin and Butcher, 2015; Minchin et al., 2018), there is no information currently about the importance or function of acetylation at K^{188}.

Deacetylation of NAT1 was catalyzed by the sirtuins SIRT1 and SIRT2 but not by SIRT3. Both SIRT1 and SIRT2 are located in the cytosol, although not exclusively, whereas SIRT3 is found in the mitochondria. The lack of any effect of TSA, a pan inhibitor of the histone deacetylases, strongly suggests that the histone deacetylases do not deacetylate NAT1, at least in the context of the current experiments. Similar to p300/CBP, SIRT1 and 2 have a broad substrate specificity, although there is a preference for lysines with a positively charged residue in the −1 position (Rauh et al., 2013). For the NAT1 K^{100} and K^{188}, this position is occupied by a lysine and an arginine, respectively.

The effect of NAT1 acetylation on enzyme activity was measured by cotransfecting cells with SIRT1 to deacetylate the protein or by treating with NAM to maximize protein acetylation. SIRT1 increased the maximum velocity of the reaction compared with NAM treatment. These results are consistent with previous studies that showed K^{100} is required for optimum binding of AcCoA, and mutations that removed the positive charge decreased AcCoA affinity (Minchin and Butcher, 2015), which is supported by the increase in K_m for AcCoA in the NAM-treated cells (Table 2). Moreover, acetylation of NAT1 altered its sensitivity to the allosteric modulator ATP. ATP appears to compete with AcCoA, and its ability to modulate NAT1 is dependent on the charge at K^{100} (Minchin et al., 2018).

Although NAT1 acetylates a range of drugs and other xenobiotics (Hein, 2002; Rodrigues-Lima et al., 2010), it also alters cell proliferation, survival, invasion, and mitochondrial function (Butcher et al., 2008; Tiang et al., 2010, 2011; Carlisle et al., 2018; Stepp et al., 2018, 2019; Wang et al., 2018; Li et al., 2019). Whether these effects are dependent on NAT1 enzyme activity is currently unknown. It would be interesting to determine whether a stable but enzymatically inactive NAT1 could rescue any of the physiologic phenotypes associated with cell growth seen after NAT1 downregulation. Such a rescue may differentiate the role of NAT1 protein levels versus enzyme activity in its cellular functions.

NAT1 joins the growing list of proteins whose activity is regulated by the reversible acetylation of surface lysines (Narita et al., 2019). These include many pharmacological receptors, metabolic enzymes, transcription factors, and regulatory proteins. In the current study, NAT1 was shown to exist in an equilibrium between an acetylated and a deacetylated state, with the possibility of monoacetylated intermediates if acetylation of K^{100} and K^{188} are indeed independent. This is summarized in Fig. 6, in which the acetylation state of NAT1 is associated with its activity and sensitivity to regulation by ATP. Under normal conditions, approximately 30% of the protein appears to exist in the acetylated state, although these estimates apply to ectopically expressed protein. If correct, the estimation suggests that a cell can increase or decrease the extent of NAT1 acetylation, and therefore its activity, depending on different physiologic cues. Changes in NAT1 activity were more sensitive to deacetylation where the metabolism of PABA increased by 70%. By contrast, increasing the acetylation state of NAT1 with NAM decreased activity by only 20% (Fig. 5F). Upregulation of the sirtuins [for example, after resveratrol treatment or caloric restriction (Chung et al., 2012)] may therefore increase NAT1 activity. Although this is a possibility, a recent pilot study in human peripheral blood mononuclear cells failed to show any effect of resveratrol on NAT1 activity (Turiján-Espinoza et al., 2018). However, there were no data to show whether the acetylation status of endogenous NAT1 was changed after treatment. This is a particularly difficult experiment to perform given the very low levels of NAT1 in most human cells and the lack of suitable antibodies for detecting and/or immunoprecipitating endogenous protein. Efforts to identify and quantify the acetylation status of endogenous NAT1 in human cells were unsuccessful, but these experiments need to be performed for a full
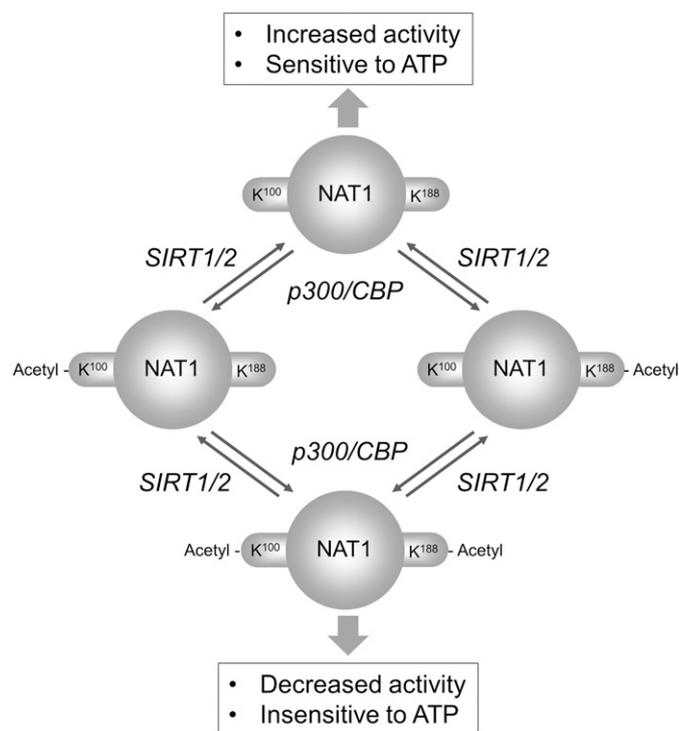
Fig. 6. Graphical representation of the equilibrium between nonacetylated, monoacetylated, or diacetylated NAT1 acetylation, enzymatic activity, and sensitivity to ATP.

understanding of the role of NAT1 acetylation in the function of the protein.

Authorship Contributions

Participated in research design: Butcher, Minchin.

Conducted experiments: Butcher, Burow.

Performed data analysis: Butcher, Minchin.

Wrote or contributed to the writing of the manuscript: Butcher, Minchin.

References

Barker DF, Husain A, Neale JR, Martini BD, Zhang X, Doll MA, States JC, and Hein DW (2006) Functional properties of an alternative, tissue-specific promoter for human arylamine N-acetyltransferase 1. *Pharmacogenet Genomics* **16**:515–525.

Butcher NJ, Arulpragasam A, Goh HL, Davey T, and Minchin RF (2005) Genomic organization of human arylamine N-acetyltransferase Type I reveals alternative promoters that generate different 5'-UTR splice variants with altered translational activities. *Biochem J* **387**:119–127.

Butcher NJ, Arulpragasam A, and Minchin RF (2004) Proteasomal degradation of N-acetyltransferase 1 is prevented by acetylation of the active site cysteine: a mechanism for the slow acetylator phenotype and substrate-dependent down-regulation. *J Biol Chem* **279**:22131–22137.

Butcher NJ, Tetlow NL, Cheung C, Broadhurst GM, and Minchin RF (2007) Induction of human arylamine N-acetyltransferase type I by androgens in human prostate cancer cells. *Cancer Res* **67**:85–92.

Butcher NJ, Tiang J, and Minchin RF (2008) Regulation of arylamine N-acetyltransferases. *Curr Drug Metab* **9**:498–504.

Carlisle SM, Trainor PJ, Doll MA, Stepp MW, Klinge CM, and Hein DW (2018) Knockout of human arylamine N-acetyltransferase 1 (NAT1) in MDA-MB-231 breast cancer cells leads to increased reserve capacity, maximum mitochondrial capacity, and glycolytic reserve capacity. *Mol Carcinog* **57**:1458–1466.

Chung JH, Manganiello V, and Dyck JR (2012) Resveratrol as a calorie restriction mimetic: therapeutic implications. *Trends Cell Biol* **22**:546–554.

Dancy BM and Cole PA (2015) Protein lysine acetylation by p300/CBP. *Chem Rev* **115**:2419–2452.

Hein DW (2002) Molecular genetics and function of NAT1 and NAT2: role in aromatic amine metabolism and carcinogenesis. *Mutat Res* **506–507**:65–77.

Husain A, Barker DF, States JC, Doll MA, and Hein DW (2004) Identification of the major promoter and non-coding exons of the human arylamine N-acetyltransferase 1 gene (NAT1). *Pharmacogenetics* **14**:397–406.

Husain A, Zhang X, Doll MA, States JC, Barker DF, and Hein DW (2007) Functional analysis of the human N-acetyltransferase 1 major promoter: quantitation of tissue expression and identification of critical sequence elements. *Drug Metab Dispos* **35**:1649–1656.

Kim SJ, Kang HS, Chang HL, Jung YC, Sim HB, Lee KS, Ro J, and Lee ES (2008) Promoter hypomethylation of the N-acetyltransferase 1 gene in breast cancer. *Oncol Rep* **19**:663–668.

Li P, Butcher NJ, and Minchin RF (2019) Arylamine N-acetyltransferase 1 regulates expression of matrix metalloproteinase 9 in breast cancer cells: role of hypoxia-inducible factor 1-α. *Mol Pharmacol* **96**:573–579.

Minchin RF and Butcher NJ (2015) The role of lysine(100) in the binding of acetylcoenzyme A to human arylamine N-acetyltransferase 1: implications for other acetyltransferases. *Biochem Pharmacol* **94**:195–202.

Minchin RF, Rosengren KJ, Burow R, and Butcher NJ (2018) Allosteric regulation of arylamine N-acetyltransferase 1 by adenosine triphosphate. *Biochem Pharmacol* **158**:153–160.

Narita T, Weinert BT, and Choudhary C (2019) Functions and mechanisms of non-histone protein acetylation. *Nat Rev Mol Cell Biol* **20**:156–174.

North BJ, Marshall BL, Borra MT, Denu JM, and Verdin E (2003) The human Sir2 ortholog, SIRT2, is an NAD+-dependent tubulin deacetylase. *Mol Cell* **11**:437–444.

Paterson S, Sin KL, Tiang JM, Minchin RF, and Butcher NJ (2011) Histone deacetylase inhibitors increase human arylamine N-acetyltransferase-1 expression in human tumor cells. *Drug Metab Dispos* **39**:77–82.

Rauh D, Fischer F, Gertz M, Lakshminarasimhan M, Bergbrede T, Aladini F, Kambach C, Becker CF, Zerweck J, Schutkowski M, et al. (2013) An acetylome peptide microarray reveals specificities and deacetylation substrates for all human sirtuin isoforms. *Nat Commun* **4**:2327.

Rodrigues-Lima F, Dairou J, Busi F, and Dupret JM (2010) Human arylamine N-acetyltransferase 1: a drug-metabolizing enzyme and a drug target? *Curr Drug Targets* **11**:759–766.

Stepp MW, Doll MA, Carlisle SM, States JC, and Hein DW (2018) Genetic and small molecule inhibition of arylamine N-acetyltransferase 1 reduces anchorage-independent growth in human breast cancer cell line MDA-MB-231. *Mol Carcinog* **57**:549–558.

Stepp MW, Salazar-González RA, Hong KU, Doll MA, and Hein DW (2019) N-acetyltransferase 1 knockout elevates acetyl coenzyme A levels and reduces anchorage-independent growth in human breast cancer cell lines. *J Oncol* **2019**:3860426.

Tiang JM, Butcher NJ, Cullinane C, Humbert PO, and Minchin RF (2011) RNAi-mediated knock-down of arylamine N-acetyltransferase-1 expression induces E-cadherin up-regulation and cell-cell contact growth inhibition. *PLoS One* **6**:e17031.

Tiang JM, Butcher NJ, and Minchin RF (2010) Small molecule inhibition of arylamine N-acetyltransferase Type I inhibits proliferation and invasiveness of MDA-MB-231 breast cancer cells. *Biochem Biophys Res Commun* **393**:95–100.

Turiján-Espinoza E, Salazar-González RA, Uresti-Rivera EE, Hernández-Hernández GE, Ortega-Juárez M, Milán R, and Portales-Pérez D (2018) A pilot study of the modulation of sirtuins on arylamine N-acetyltransferase 1 and 2 enzymatic activity. *Acta Pharm Sin B* **8**:188–199.

Wang L, Minchin RF, and Butcher NJ (2018) Arylamine N-acetyltransferase 1 protects against reactive oxygen species during glucose starvation: role in the regulation of p53 stability. *PLoS One* **13**:e0193560.

Wu H, Dombrovsky L, Tempel W, Martin F, Loppnau P, Goodfellow GH, Grant DM, and Plotnikov AN (2007) Structural basis of substrate-binding specificity of human arylamine N-acetyltransferases. *J Biol Chem* **282**:30189–30197.

Zhang X, Carlisle SM, Doll MA, Martin RCG, States JC, Klinge CM, and Hein DW (2018) High N-acetyltransferase 1 expression is associated with estrogen receptor expression in breast tumors, but is not under direct regulation by estradiol, 5α-androstane-3β,17β-Diol, or dihydrotestosterone in breast cancer cells. *J Pharmacol Exp Ther* **365**:84–93.

Address correspondence to: Dr. Neville J. Butcher, School of Biomedical Sciences, University of Queensland, St Lucia, QLD 4072, Australia. E-mail: n.butcher@uq.edu.au